ACS Chemical Neuroscience

Research Article

pubs.acs.org/chemneuro

sym-Triazines for Directed Multitarget Modulation of Cholinesterases and Amyloid-β in Alzheimer's Disease

Anthony J. Veloso,[†,§] Devjani Dhar,[†,§] Ari M. Chow,[‡] Biao Zhang,[†] Derek W. F. Tang,[‡] Hashwin V. S. Ganesh,[‡] Svetlana Mikhaylichenko,[†] Ian R. Brown,[‡] and Kagan Kerman*[,†,‡]

[†]Department of Physical and Environmental Sciences, and [‡]Centre for the Neurobiology of Stress, Department of Biological Sciences, University of Toronto Scarborough, 1265 Military Trail, Toronto, Ontario M1C 1A4, Canada

Supporting Information

ABSTRACT: Alzheimer's disease (AD) is a complex neurodegenerative disorder marked by numerous causative factors of disease progression, termed pathologies. We report here the synthesis of a small library of novel *sym*-triazine compounds designed for targeted modulation of multiple pathologies related to AD, specifically human acetylcholinesterase (AChE), butyrylcholinesterase (BuChE), and Aβ aggregation. Rational targeting of AChE was achieved by the incorporation of acetylcholine substrate analogues into a *sym*-triazine core in either a mono-, di-, or trisubstituted regime. A subset of these derivatives demonstrated improved activity compared to several commercially available cholinesterase inhibitors. High AChE/BuChE selectivity was characteristic of all derivatives, and AChE steady-state kinetics indicated a mixed-type inhibition mechanism. Further integration of multiple hydrophobic phenyl units allowed for improved β-sheet intercalation into amyloid aggregates. Several highly effective structures exhibited fibril inhibition greater than the previously reported β-sheet-disrupting penta-peptide, iAβ5p, evaluated by thioflavin T fluorescence spectroscopy and transmission electron microscopy. Highly effective *sym*-triazines were shown to be well tolerated by differentiated human neuronal cells, as demonstrated by the absence of adverse effects on cellular viability at a wide range of concentrations. Parallel targeting of multiple pathologies using *sym*-triazines is presented here as an effective strategy to address the complex, multifactorial nature of AD progression.

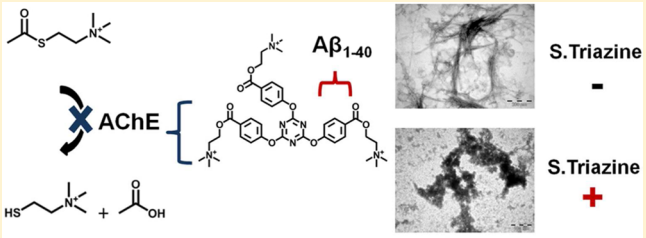

KEYWORDS: *Alzheimer's disease, amyloid-β, acetylcholinesterase, inhibitor, butyrylcholinesterase, sym-triazine*

Alzheimer's disease (AD) is the most prevalent form of age-related dementia characterized by progressive, irreversible impairments to memory[1,2] and cognitive functions.[3,4] Pathological deterioration of AD patients has been strongly associated with the overproduction and disregulation of the amyloid-beta (Aβ) peptide.[5] Aβ has been implicated in a number of neurotoxic pathways related to the formation of reactive oxygen species,[6] the disruption of Ca^{2+} homeostasis[7] and chronic activation of microglia.[8] One prominent strategy to reduce neurodegeneration has thus emphasized the removal of neurotoxic Aβ oligomers by implementing small-molecule aggregation modulators that disrupt $\pi-\pi$ stacking between β-sheets in order to impede Aβ self-association.[9,10] Although the development and commercialization of Aβ-modulating agents are underway,[11,12] currently available pharmacological treatments have targeted more distal pathways of neurodegeneration, which are limited to two classes of compounds: *N*-methyl-D-aspartate (NMDA) receptor antagonists and cholinesterase inhibitors (ChEIs).[13] The aim of such drug therapies is not to impede the proposed aetiopathologies but rather to ameliorate behavioral and cognitive dysfunctions, which have significantly delayed and in some cases avoided the need for institutionalization.[14]

In particular, cognitive dysfunction has been associated with the deterioration of cholinergic neurons of the basal forebrain and neocortex, leading to profound deficits in the production of the neurotransmitter, acetylcholine.[15] Accordingly, ChEIs have been implemented effectively to restore pathologically reduced neurotransmitter levels by modulating native hydrolytic degradation catalyzed by the enzyme, acetylcholinesterase (AChE).[16] Currently, four ChEIs have been approved by the FDA for clinical treatment of mild to severe stage AD. These include: galanthamine (REMINYL), rivastigmine (EXELON), tacrine (COGNEX) and donepezil (ARICEPT).[17,18] In view of the limited number of commercially available drug therapies for AD, continued progression toward more biologically compatible ChEI is imperative.

Further motivation for the synthesis of novel ChEI has stemmed from the recent identification of AChE as an accelerant of Aβ aggregation via interaction with the peripheral anionic site (PAS) of the enzyme. This has been further confirmed by studies with butyrylcholinesterase (BuChE), a nonspecific cholinesterase variant that lacks a PAS, which is

Received: October 2, 2012
Accepted: October 30, 2012
Published: October 30, 2012

Scheme 1. Synthetic Routes for New Ester and Ester-Salt *sym*-Triazine Derivatives[a]

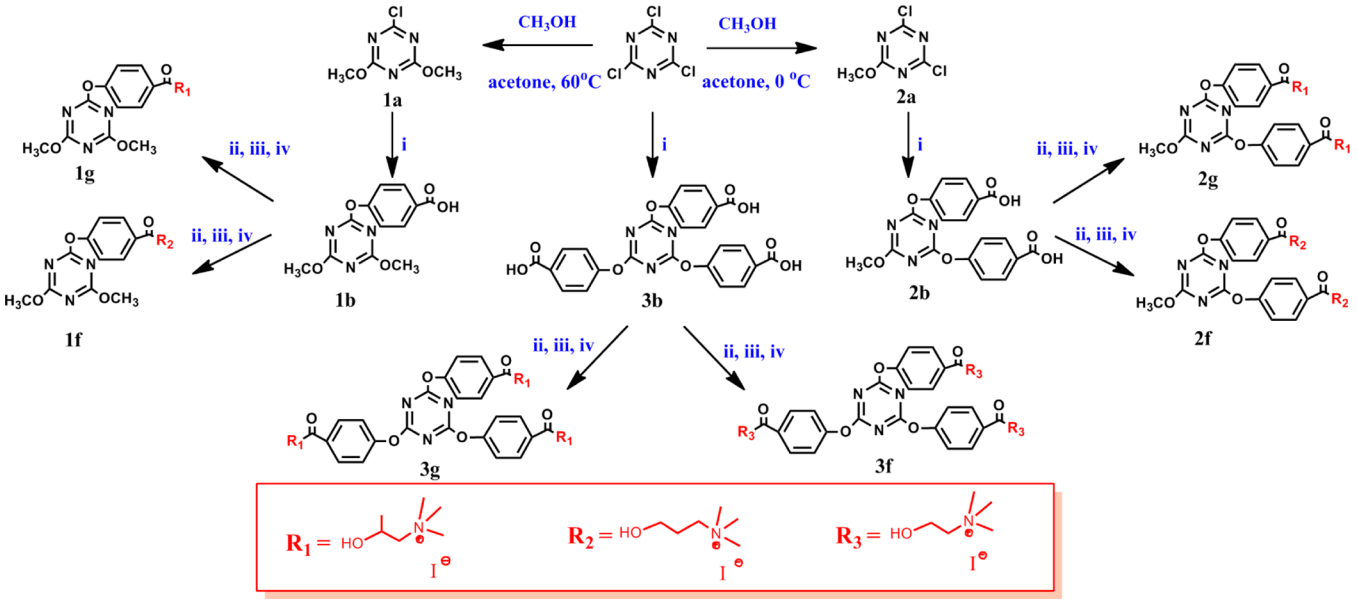

[a](i) Reactions were run using oxybenzoic acid, NaOH, and water in acetone. Acidification was performed using concentrated HCl to yield **1b**, **2b**, and **3b**. (ii) Reactions were run at 60°C in $SOCl_2$ using anhydrous $CHCl_3$ as solvent and pyridine as catalyst. (iii) Reactions were carried out using 3-dimethylamino-1-propanol, 1-dimethylamino-2-propanol, and 2-dimethylaminoethanol in anhydrous THF in the presence of triethylamine as the base. (iv) Reactions were carried out at 40°C using iodomethane in anhydrous THF.

unable to induce such accelerated growth.[19] Rivastigmine is a pseudo-irreversible inhibitor that binds to the catalytic active site region forming a carbamylated enzyme intermediate that dissociates slowly. Conversely, donepezil, tacrine, and gallanthamine are rapidly reversible inhibitors capable of only short-term interaction with the AChE PAS.[20,21] Notably, certain PAS-binding ChEI, such as donepezil, have been shown to impede AChE-induced Aβ aggregation, thereby prompting the development of a novel class of ChEI capable of mediating long-term beneficial changes.[22] Combination targeting of distinct AD pathologies using multiple, independently acting drug therapies has emerged as a highly potent strategy to address the complex, degenerative nature of AD. Combination studies of ChEI have a synergistic enhancement of therapeutic effects compared to single drug therapies.[23] However, the implementation of multiple single-drug entities also raises a potential for conflicting bioavailabilities, pharmacokinetics, and metabolism between compounds.[24,25] More recent innovations have sought to address these concerns through the incorporation of multiple pharmacophores into single drug entities, which still retain the ability of each individual component to interact with its intended target.[26] Multitargeted therapies are also expected to simplify therapeutic regimens for patients leading to improved applicability for AD care. An approach in multitarget drug therapy development for AD is to integrate a ChEI pharmacophore with a second unit capable of targeting a separate AD pathology.[27−30] Herein, we report for the first time a library of novel *sym*-triazine-derived compounds capable of parallel modulation of Aβ aggregation and AChE/BuChE hydrolytic activity.

RESULTS AND DISCUSSION

Synthesis of *sym*-Triazine Derivatives. Most reactions of *sym*-triazines are nucleophilic substitutions of chloro-triazines, in particular, 2,4,6-trichloro-1,3,5-triazine (cyanuric chloride, CC).[31,32] CC is often used as a starting material due to the facile displacement of its chlorine atoms, which has been demonstrated using a number of nucleophiles in the presence of hydrochloride acceptors such as sodium carbonate, sodium bicarbonate, and sodium hydroxide.[33] CC is especially advantageous as it decreases in reactivity with successive substitutions.[34,35] Consequently, the number of arm substitutions can be controlled by various factors including reaction duration, solvent and base strength, the nucleophilic structure, steric factors, and substituents already present in the *sym*-triazine ring. Temperature is a primary factor governing CC substitutions. Generally monosubstitutions were performed at approximately 4 °C, disubstitutions at room temperature, and trisubstitutions above 60 °C. The commercial availability and low cost of CC render it a practical choice for the synthesis of *sym*-triazine derivatives.[34,36]

Initial derivatization of cyanuric chloride (CC) involved the incorporation of methoxy groups (**1a** and **2a**) via nucleophilic aromatic substitution of chlorine with methanol, following procedures established by Dudley (Scheme 1).[37] Methanol substitution was integral for controlling the number of Aβ- and AChE-targeted substitutions within the triazine core. Accordingly, the synthesis of **2a** was performed at 0 °C in order to displace only a single chlorine unit in the triazine ring of CC, leaving two chlorine units available for further derivatization forming the targeted disubstituted species. Similarly, the synthesis of **1a** required reaction temperatures of 60 °C for the displacement of two chlorine units, leaving a single unit available for derivitization of a monosubstituted triazine. The resulting products were washed with water to eliminate inorganic salts formed during the reaction. The *sym*-triazine-based carboxylic acids, **1b** and **2b**, were subsequently synthesized from the methoxy derivatives, **1a** and **1b**, respectively, using 4-oxybenzoic acid reported by Pogosyan et al.[38] The trisubstituted acid, **3b**, was directly synthesized from a reaction of 4-oxybenzoic acid with CC following conditions and

dx.doi.org/10.1021/cn300171c | ACS Chem. Neurosci. 2013, 4, 339−349

Chart 1. *sym*-Triazine Derivatives Incorporating Acetylcholine-Like Substitutions for Multi-Targeted Inhibition of AChE, BuChE, and Aβ Aggregation

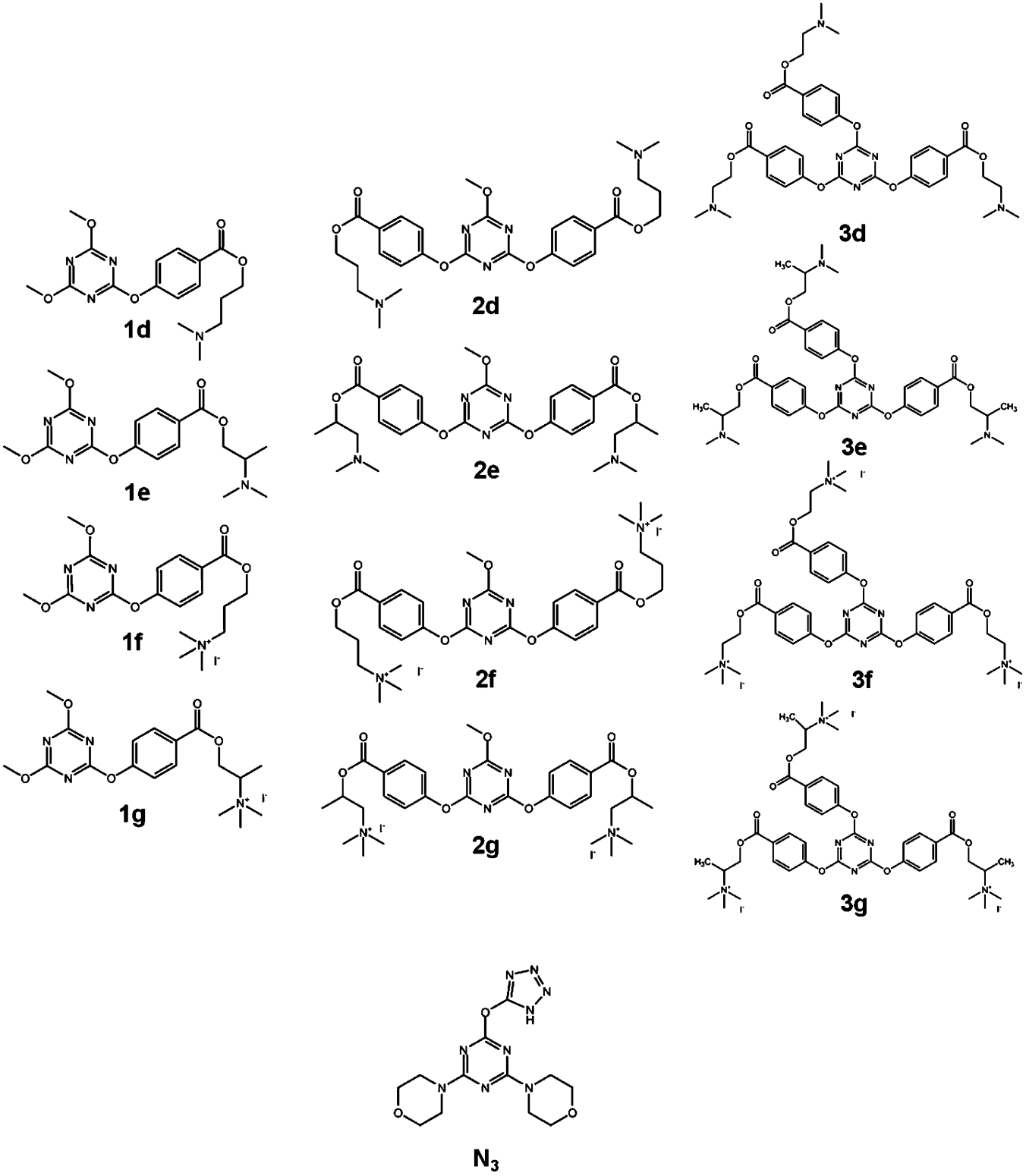

procedures developed by Sklyarskii et al.[39] Sodium hydroxide was employed as a base to synthesize oxybenzoate salts of **1a**, **2b**, and **3b** followed by the addition of dilute HCl to the salt solution. Notably, we have observed that Aβ aggregation could be severely impaired *in vitro* by the presence of hydrophobic poly aromatic compounds, which are capable of disrupting or preventing $\pi-\pi$ stacking. Thus, the addition of multiple aromatic functional units by substitution with oxybenzoate salts was performed for rational targeting of Aβ aggregation.

The synthesis of the acyl chloride compounds **1c**, **2c**, and **3c** from **1b**, **2b**, and **3b**, respectively, by a nucleophilic acyl substitution reaction involved replacement of the hydroxy

dx.doi.org/10.1021/cn300171c | *ACS Chem. Neurosci.* 2013, 4, 339−349

Table 1. Analysis of AChE, BuChE, and Aβ Inhibition *in Vitro* by *sym*-Triazine Derivatives

compd	yield (%)	IC_{50} AChE (μM)	IC_{50} BuChE (μM)	IC_{50} ratio BuChE/AChE	% inhibition Aβ fibrils 2×[i][a]	% inhibition Aβ fibrils 1×[i][a]
1d	68.6	89.8 ± 2.9	>200		48.3	5.5
1e	41.6	56.4 ± 1.7	>200		46.6	6.6
1f	88.0	38.8 ± 1.4	>200		28.8	34.2
1g	74.2	18.4 ± 1.3	>200		25.2	31.3
2d	53.5	171.5 ± 8.6	>200		71.3	42.3
2e	34.2	110.5 ± 4.3	>200		88.2	58.4
2f	38.7	20.3 ± 1.5	>200		75.2	41.8
2g	44.4	9.7 ± 0.4	>200		95.2	65.6
3d	17.0	9.8 ± 0.2	13.9 ± 0.3	1.4	67.9	53.2
3e	64.4	80.8 ± 2.9	163.8 ± 7.7		87.4	68.5
3f	68.0	0.3 ± 0.02	3.9 ± 0.2	13.0	70.2	50.9
3g	89.1	2.8 ± 0.1	15.3 ± 0.9	5.5	89.9	72.1
N_3	82.1	153.2 ± 12.7	>200			
donepezil	23.0	0.02 ± 0.004	4.0 ± 0.4	200.0		
iAβ5p					58.5	28.6

[a]Measured with 100 μM $Aβ_{1-40}$ incubated with 200 μM (2×) or 100 μM (1×) inhibitor ([i]) at 37 °C for 72 h in 50 mM PBS (pH 7.4).

groups of the carboxylic acids with chlorine functional units. To accomplish this, the carboxylic acid derivatives were treated with thionyl chloride using anhydrous chloroform as the solvent with a pyridine catalyst. IR spectroscopic data indicated the formation of the acyl chloride by a shift of carbonyl and carboxyl absorption peaks as well as the disappearance of the hydroxyl peak. The resulting acyl chlorides were unstable hygroscopic species that could be easily converted back to their corresponding carboxylic acid derivatives simply by exposure to air. As a result, esterification was performed immediately following the formation of the acyl chlorides by nucleophilic addition−elimination with various combinations of the following compounds: 1-dimethylamino-2-propanol, 3-dimethylamino-1-propanol, and 2-dimethylaminoethanol. These compounds were designed as analogues of the native enzyme substrate, acetylcholine, and were thus incorporated into the triazine structure for functional targeting of the AChE active site. All compounds demonstrated moderate to high conversion to the esters except for one due to the different temperature conditions employed. Compound **3c** reacted with 2-dimethylaminoethanol at a temperature maintained at 15 °C, which generated the ester, **3d**, in a poor isolated yield of 17%. Hence, reaction conditions were optimized for the formation of esters **1d**, **1e**, **2d**, **2e**, and **3d** by carrying out their synthesis at 40 °C. The triethylamine hydrochloride salt formed during these esterification reactions was eliminated from the solvent tetrahydrofuran (THF) comprising the ester. For each esterification reaction, a brown, viscous oil resulted after the evaporation of THF, which was washed several times with water to allow the esters to precipitate. Water was eliminated to obtain the solid esters **1d**, **1e**, **2d**, **2e**, **3d**, and **3e** in 68.6, 41.6, 53.5, 34.2, 17.0, and 64.4% yields, respectively.

Further electrophilic substitution of the ester products with iodomethane was used to generate a series of novel iodine-ester salts, **1f** in 88.0% yield; **1g** in 74.2% yield; **2f** in 38.7% yield; **2g** 44.4% yield; **3f** in 68.0% yield; and **3g** in 89.1% yield. Compounds **1g**, **2g**, and **3g** were isolated as stereoisomers. Reactions for all compounds synthesized were monitored using thin layer chromatography (TLC) in 1:1 acetone and hexane solution, and structures were confirmed using IR, MS, ^{1}H NMR, and ^{13}C NMR (see Supporting Information).

Cholinesterase Inhibition Studies. The inhibitory effects of 12 novel *sym*-triazine derivatives (Chart 1) on AChE activity was characterized using Ellman's colorimetric assay,[22,29,40,41] in which AChE-catalyzed hydrolysis was initiated in the presence of a chromogenic agent, 5,5′-dithiobis (2-nitrobenzoic acid) (DTNB). Enzyme activity was determined by comparing the rate of substrate hydrolysis (ΔOD_{410}/min) in the presence and absence of inhibitor. The AChE IC_{50} values for all *sym*-triazines are reported in Table 1 and correspond to the concentration of inhibitor that resulted in a 50% reduction of enzyme activity. The IC_{50} of each compound was derived from nonlinear regression of AChE activity plots performed over a range of inhibitor concentrations. Clinically established cholinesterase inhibitor (ChEI), donepezil, was implemented as a positive control for AChE inhibition. The AChE IC_{50} for donepezil was determined to be approximately 0.02 μM, in agreement with previously reported values.[29,42]

Substantial enhancement of inhibitor activity was achieved via three rational modifications of the triazine core: (1) the incorporation of acetylcholine substrate analogues as terminal substituents of the triazine branches, (2) the conversion of terminal amine groups to positively charged quaternary amine iodide salts, and (3) by increasing the number of analogue-containing branches from 1 to 3. Specifically, we characterized the effects of three types of acetylcholine-like branch derivatives (Scheme 1, red box) possessing either an additional methyl subunit (R_1), an elongated alkyl chain (R_2), or an exact structural analogue of acetylcholine (R_3). Notably, the elongated chains of R_2 were found to significantly reduce inhibition activity, resulting in much higher IC_{50} values. However, this was not attributed to the increased hydrophobicity introduced by the alkyl chain unit since the activity of the methyl substituent-containing R_1-triazines showed inhibitory effects comparable to those of R_3. One possibility is that the triazine core plays a critical role in blocking the enzyme active site, and the additional carbon chain of R_2 creates a sufficiently large gap for the substrate to enter. In general, the branch activity in order of most effective to least effective inhibitor of AChE was determined to be $R_3 > R_1 > R_2$.

Subsequent incorporation of positive charges through conversion of *sym*-triazines to quaternary amine salts enhanced inhibition by increasing the electrostatic binding affinity toward the negatively charged peripheral anionic site (PAS). As expected, quaternary amine-modified monosubstituted triazines (**1f** and **1g**) presented greater inhibition (>50% drop in IC_{50})

compared to that of their underivatized counterparts (**1d** and **1e**). As a result, iodide salt-conversion was performed for di- and trisubstituted *sym*-triazines. All quaternary amines (designated **f** or **g**) exhibited drastic improvements to inhibition from increasing arm substitutions, with trisubstituted compounds, **3f** and **3g**, resulting in the most profound inhibition of AChE activity (IC_{50} of 0.3 μM and 2.8 μM, respectively). In comparison, underivatized *sym*-triazines (designated **d** or **e**) showed only comparable or even reduced inhibition with increased branching from 1 to 3. A negative control lacking the acetylcholine-like substitutions, N_3 (Chart 1), showed lower activity (IC_{50} of 153.3 μM) than the least effective quaternary-amine-based *sym*-triazine, **1f** (IC_{50} of 38.8 μM), thus emphasizing the relevance of positive charge in addition to acetylcholine-like structures for enhancing targeted inhibition of AChE. AChE inhibition plots of the most effective compounds, **2g**, **3f**, and **3g**, are shown in Figure 1a. In regard to the current FDA

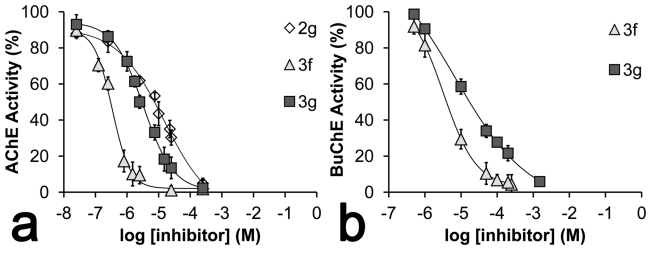

Figure 1. Inhibition plots of (a) AChE (**2g**, **3f**, and **3g**) and (b) BuChE (**3f** and **3g**) activity in the presence of increasing concentrations of *sym*-triazine derivatives as determined by Ellman's method. Error bars denote the standard deviation for $n \geq 3$.

approved ChEI, all three compounds as well as **3d** were characterized by IC_{50} lower than rivastigmine (IC_{50} > 10 μM).[42] Notably, **3f** (IC_{50} of 300 nM) demonstrated stronger inhibition than galanthamine (IC_{50} of 575 nM)[42] and was surpassed only by donepezil (IC_{50} of 20 nM)[42] in activity.

Inhibition of AChE-catalyzed hydrolysis involves ligand interaction with either the catalytic active site or by allosteric modulation of the PAS.[43] Butyrylcholinesterase (BuChE) is a variant of the cholinesterase enzyme, in which the absence of several key aromatic residues at the PAS results in significantly lowered binding affinity toward typical PAS-targeting ligands.[44] Consequently, *sym*-triazine binding site selectivity could be discriminated through comparative BuChE inhibition assays. Analysis of BuChE IC_{50} (Table 1) indicated that all compounds possessed substantially higher AChE selectivity (i.e., lower IC_{50}), suggesting that interaction with the PAS was critical to *sym*-triazine-mediated cholinesterase inhibition. The most effective BuChE inhibitors, **3f** and **3g** (Figure 1b), exhibited activity (BuChE IC_{50} of 3.9 μM and 15.3 μM, respectively) similar to that of donepezil (BuChE IC_{50} of 4.0 μM). Comparing the inhibitory effects of acetylcholine analogues, we found that R_3 compounds (**3d** and **3f**) showed higher affinity for the BuChE active site over the methyl modified R_1 triazines (**3e** and **3g**). Increasing the number of analogue branches was also found to significantly improve the active site inhibition, resulting in substantially lower BuChE IC_{50}. High PAS affinity has been associated with suppression of AChE-accelerated Aβ fibril formation[22] specifically for compounds that bind via a noncompetitive, mixed mechanism of inhibition. Therefore, kinetic analysis of AChE (Figure S1, Supporting Information) was also performed for highly effective *sym*-triazines **2d**, **3d**, **3f**, and **3g**. Graphical analysis of double reciprocal plots (Figure S1a–d, Supporting Information) showed increased slopes with increasing inhibitor concentration as well as intersecting intercepts beyond the *y*-axis, indicative of mixed-type inhibition.[41] Data replots (Figure S1e–h, Supporting Information) were used to determine the inhibitor constants (Table 2) denoted by the *x*-intercept.

Table 2. Competitive Inhibition Constants (K_i) of Highly Effective *sym*-Triazine Derivatives for AChE

AChE	
compd	K_i (μM)
2g	4.31
3d	4.92
3f	1.62
3g	1.49
donepezil	0.01

Inhibition of Aβ_{1-40} Aggregation. Targeting of Aβ aggregation was achieved primarily through the addition of multiple aromatic phenyl groups proximal to the triazine core. Thus, a significant reduction of Aβ_{1-40} aggregation was observed by Thioflavin T (ThT) fluorescence, as the number of phenyl-containing substitutions was increased between mono- and trisubstituted derivatives (Table 1). The additional methyl substitution of **3g** resulted in approximately 20% improvement in the inhibition of fibril formation compared to **3f**. It is suggested that additional methyl subunits provided a greater hydrophobic component that enhanced the capacity to intercalate between the β-sheets.[45,46] Sym-triazine derivatives possessing 2–3 arm substitutions showed greater than 70% inhibition after 3 days of incubation at 37 °C at 2× the concentrations. This measured activity was substantially greater than that of the established penta-peptide-based β-sheet breaker, iAβ5p (58.5%). ThT studies also confirmed that donepezil exhibited a near negligible effect on amyloid aggregation (6.9%), further highlighting the significance of rational *sym*-triazine functionalization for β-sheet targeting.

Transmission electron microscopy (TEM) studies confirmed the inhibition of fibril formation using quaternary amine-salt converted *sym*-triazines **2f**, **2g**, **3f**, and **3g** as well as iAβ5p, measured after 4 days of incubation (Figure 2). Aβ_{1-40} controls showed distinct fibrillar networks of defined elongated structure in the absence of *sym*-triazines. As also observed in ThT studies, donepezil appeared to demonstrate no observable effect on the fibril elongation process. While in the presence of a known inhibitor, iAβ5p, a mixture of both globular aggregates and fibrils was observed, suggesting incomplete inhibition concurrent with fluorescence data. This was further supported by the observed length of iAβ5p-treated fibrils, which were significantly truncated relative to the uninhibited controls. Conversely, Aβ_{1-40} samples containing *sym*-triazines exhibited only globular features lacking a defined fibrillar component. The lack of Aβ_{1-40} fibrils was supported by a significantly reduced ThT fluorescence emission at 485 nm relative to the Aβ_{1-40} control. Previously, a number of Aβ-targeting therapies focused largely on the disassembly or inhibition of Aβ fibril formation.[47] However, this particular strategy for Aβ-inhibition has received much criticism as the decrease in fibrillar content would lead to an increased concentration of the more toxic soluble species of Aβ.[48] Alternatively, amyloid-targeting agents such as EGCG and various flavonoid compounds modulate Aβ

dx.doi.org/10.1021/cn300171c | ACS Chem. Neurosci. 2013, 4, 339–349

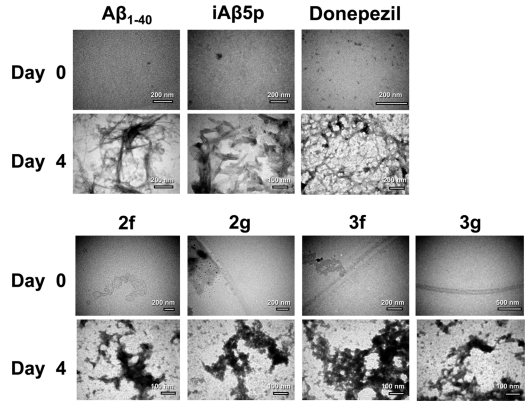

Figure 2. Transmission electron micrographs of inhibited Aβ_{1-40} fibril growth measured *in vitro* at 0 and 4-day incubations of 100 μM Aβ_{1-40} in the presence and absence of *sym*-triazine derivatives **2f**, **2g**, **3f**, and **3g** (200 μM) at 37 °C. Well-described β-sheet disrupter, iAβ5p (200 μM), and AChE inhibitor, donepezil (200 μM), were employed as controls for fibril inhibition.

activity by forcing the peptide to deviate from conventional fibrillar architecture in favor of off-pathway amorphous globular aggregate states that have been found to be benign in toxicity.[49−51] It has been further suggested that the formation of these benign amorphous aggregates could serve to be additionally beneficial as they would function as potential sinks for soluble Aβ oligomers.[52] We observed that the tested *sym*-triazine derivates stimulated the formation of globular aggregates over fibrillar structures, though the toxicity of the resulting aggregates requires further study.

Comparatively, TEM analysis of underivatized triazines, **2d**, **2e**, **3d**, and **3e** (Figure S2, Supporting Information), showed globular formations similar to those seen for their quaternary amine counterparts, in which the lack of fibrillar features was also confirmed by a reduced ThT fluorescence emission. The results indicated that the charges of the amine units did not significantly affect the capacity of the triazines to impede fibril assembly. We report for the first time the formation of nonfibrillar amorphous Aβ aggregates in the presence of our novel *sym*-triazine derivatives, highlighting the promising potential of these *sym*-triazines for targeted inhibition of Aβ aggregation.

Collective analysis of all tested *sym*-triazine compounds revealed that **3f** and **3g** distinctly exhibited high activity in regard to multitargeted inhibition of both AChE and Aβ

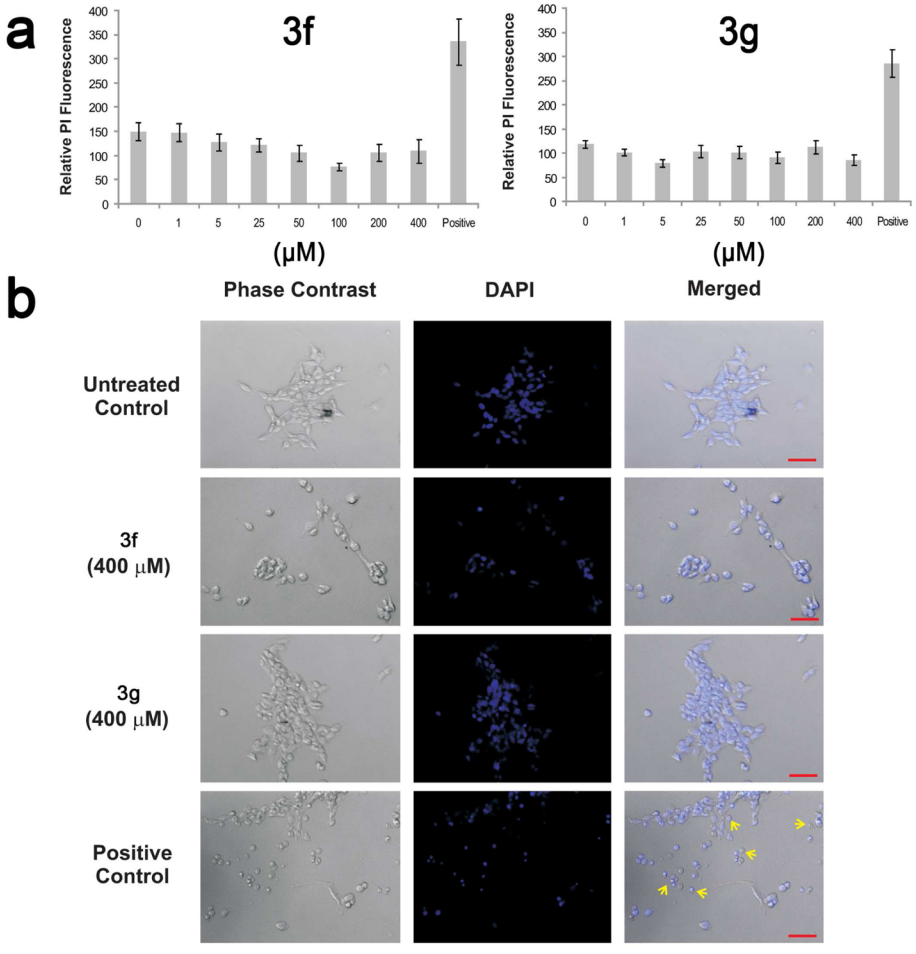

Figure 3. Multitarget *sym*-triazine inhibitors **3f** and **3g** were tolerated by differentiated human neuronal cells. (a) Quantitative assay for the viability of cells was examined by propidium iodide (PI) exclusion methodology as described in the Methods section. (b) Morphology of cells treated with 400 μM of **3f** or **3g** for 24 h was examined with phase contrast and epifluorescence (DAPI counter staining) microscopy. Only the positive control (treatment with toxic dosage of celastrol at 3 μM)[55] demonstrated dead cells showing extensive rounding of the cell body and condensation of nuclei, as indicated by yellow arrows. Phase contrast and epifluorescence images were obtained using an AxioCam HRm camera on an AxioVert 200 M microscope (Carl Zeiss) with a X20 objective. Scale bar = 100 μm.

dx.doi.org/10.1021/cn300171c | *ACS Chem. Neurosci.* 2013, 4, 339−349

pathologies. Compounds **3f** and **3g** possess the maximum number of quaternary amine-derivatized acetylcholine substitutions and thus served as effective structures to be used for comprehensive assessment of the *sym*-triazines' impact on live cells. The propidium iodide (PI) exclusion assay demonstrated that the viability of differentiated SH-SY5Y human neuronal cells was not affected with treatment of up to 400 μM of **3f** or **3g** (Figure 3), demonstrating a tolerable threshold well above the dosages required in this study for effective inhibition of AChE activity. Fluorescence microscopy demonstrated the absence of cell death morphology in differentiated human neuronal cells treated with 400 μM **3f** or **3g** compared to controls in which cell death was induced by toxic levels of celastrol[43] (Figure 3). The results further emphasized the applicability of these *sym*-triazines to biological samples, demonstrating a promising potential for further preclinical investigations.

Multitargeted drug therapies are an innovative approach to address the complex and inter-related nature of AD pathologies. We presented the structure−activity studies of a novel class of *sym*-triazine-based therapies for AD capable of multitargeted inhibition of both AChE activity and Aβ aggregation *in vitro*. Rational optimization of triazines resulted in progressive enhancement of activity through successive derivitization. Improved targeting of AChE was achieved through direct incorporation of structural analogues of the native substrate, acetylcholine. Additional directed inhibition of Aβ self-assembly was achieved via the integration of multiple, hydrophobic phenyl units that disrupted $\pi-\pi$ stacking. Several disubstituted and trisubstituted *sym*-triazine derivatives possessed comparable or greater activity compared to those of several commercially available inhibitors with regard to the modulation of both AChE and Aβ activity. Compounds **2g**, **3d**, **3f**, and **3g** demonstrated a mixed-type mechanism of inhibition and high PAS affinity, which has been associated with the capacity to impede AChE-accelerated Aβ fibril formation. Cell viability studies showed that **3f** and **3g** were well tolerated by differentiated human neuronal cells. Our design of *sym*-triazines with acetylcholine-like substitutions has generated hybrid molecules that possess multiple beneficial activities to be used as potential candidates for AD therapies.

METHODS

Thin-layer chromatography (TLC) was performed on Merck Silica Gel 60 F_{254}, 20 × 20 cm plates and visualized using a 254 nm UV lamp. ^{1}H NMR spectra (400 MHz) and ^{13}C NMR (100 MHz) spectra were recorded on Bruker Avance III using solvents DMSO-d_6, D_2O, and $CDCl_3$ and were internally referenced to residual protic solvent signals (δ 2.50, 4.79, and 7.26 δ, respectively). Data for ^{1}H NMR are reported as chemical shift (δ ppm), multiplicity (s = singlet, d = doublet, t = triplet, q = quartet, m = multiplet, and dd = doublet of doublets), J coupling constant (Hz), and assignment. Data for ^{13}C NMR are reported as chemical shift (δ ppm). IR spectra were recorded on a Bruker Alpha-P spectrometer with ATR attachment and reported in terms of frequency of absorption (cm^{-1}). Mass spectra were obtained using an AB/Sciex QStar mass spectrometer (ESI-TOF). Melting points were recorded on a melting point apparatus (Fisher Scientific). Reagents were obtained from commercial vendors and used as received unless otherwise noted.

Procedures for the Preparation of *sym*-Triazine Based Acids. *4-((4,6-Dimethoxy-1,3,5-triazin-2-yl)oxy)benzoic Acid (**1b**) and 4,4′-((6-Methoxy-1,3,5-triazine-2,4-diyl)bis(oxy))dibenzoic Acid (**2b**).* Compounds **1b** and **2b** were synthesized following the previously reported procedure by Pogosyan et al.[38]

*2,4,6-Tris (4′-Chlorocarbonylphenoxy)-1,3,5-triazine (**3b**).* Compound **3b** was produced in one step by CC and 4-oxybenzoic acid; applying the previously reported method by Sklyarskii et al.[39]

Procedure for *sym*-Triazine Based Acyl Chlorides. *4-((4,6-Dimethoxy-1,3,5-triazin-2-yl)oxy)benzoyl Chloride (**1c**) (Procedure A).* A mixture of 11 g of **1b** (0.04 mol), 8.82 mL of thionyl chloride (0.12 mol), and one drop of pyridine in 100 mL of dry chloroform was refluxed and boiled for 6 h. The reaction was monitored by thin layer chromatography (TLC) for completion. Chloroform was distilled off at 60 °C until the solution started to turn light yellow. Then, 120 mL of petroleum ether was added to the solution and allowed to precipitate for an hour. The white precipitate was washed with petroleum ether. The white solid had a melting point of 105−107 °C with a 60.6% final yield.

IR (neat) ν = 3072.00, 1771.45, 1746.00, 1564.14, 1468.49, 1199.02, 806.35 cm^{-1}; ^{1}H NMR (400 MHz, $CDCl_3$) δ 8.21−8.19 (d, J = 8.9 Hz, 2 H), 7.36−7.34 (d, J = 8.9 Hz, 2 H), 4.02 (s, 6 H); ^{13}C NMR (100.42 MHz, $CDCl_3$) δ 174.1, 173.0, 167.9, 157.1, 133.4, 121.5, 55.9. Calculated $C_{12}H_{10}N_3O_4Cl$ ($[M + H]^+$), 295.68; found, 296.0.

*4,4′-((6-Methoxy-1,3,5-triazine-2,4 diyl)bis(oxy))dibenzoyl Chloride (**2c**).* Compound **2b** (5 g (0.01 mol)), 11.25 mL (moles) of thionyl chloride, and one drop of pyridine in 100 mL of dry chloroform were heated until boiling for 6 h. Procedure A was followed to provide **2c** in 79.8% yield as a yellow powder with a melting range of 133−135 °C.

IR (neat) ν = 3076.93, 1744.13, 1560.86, 1496.04, 1197.93, 815.30 cm^{-1}; ^{1}H NMR (400 MHz, $CDCl_3$) δ 8.21−8.19 (d, J = 8.8 Hz, 4 H), 7.35−7.33 (d, J = 8.8 Hz, 4 H), 3.98 (s, 3 H); ^{13}C NMR (100.42 MHz, $CDCl_3$) δ 172.8, 169.0, 167.8, 157.0, 133.8, 131.7, 121.4, 56.5. Calculated $C_{18}H_{11}N_3O_5Cl_2$ ($[M + H]^+$), 420.2; found, 420.1.

*2,4,6-Tris(4′-chlorocarbonylphenoxy)-1,3,5-triazine (**3c**).* A mixture of 4.894 g (0.01 mol) of **3b** and 43.5 mL (0.60 mol) of thionyl chloride in 80 mL of dry chloroform and 3 drops of dry pyridine (catalyst) was refluxed under dry conditions. Procedure A was followed to provide **3c** as a light yellow powder with 185−188 °C melting point and a final yield of 88.7%.

IR (neat) ν = 3104.12, 3072.42, 2959.68, 1779.22, 1737.69, 1605.56, 1560.83, 1495.84, 1209.39, 1193.58, 1167.44,1085.77,1016.88, 821.15; ^{1}H NMR (400 MHz, $CDCl_3$) δ 8.19−8.17 (d, J = 8.8 Hz, 6H), 7.32−7.29 (d, J = 8.8 Hz, 6H); ^{13}C NMR (100.42 MHz, $CDCl_3$) δ 173.4, 167.0, 158.3, 133.5, 131.8, 122.0. Calculated $C_{24}H_{12}N_3O_6Cl_3$ ($[M + H]^+$), 544.8; found, 545.0.

Procedure for *sym*-Triazine Based Esters. *3-(Dimethylamino)-propyl-4-((4,6-dimethoxy-1,3,5 triazin-2-yl)oxy)benzoate (**1d**) (Procedure B).* Compound **1c** (2.0 g) was dissolved in 40 mL of dry THF. A solution of 6.76 mmol (0.94 mL) of dry triethylamine and 6.76 mmol (0.80 mL) of 3-dimethylamino-1-propanol in 10 mL of dry THF was added dropwise to the **1c** solution. The reaction was refluxed and the temperature maintained at 40 °C. The reaction was monitored by TLC for completion. The ester slurry was gravity filtered and washed with 3 × 6 mL of dry THF. The combined filtrate was evaporated under vacuum conditions. Then, 50 mL of dichloromethane was used to dissolve the ester residue. The dichloromethane layer was washed with 6 × 50 mL water, and the organic layer was collected. The ester solution was dried with anhydrous Na_2SO_4 overnight. The resulting residue was washed with small portions of petroleum ether (40−60 °C) resulting in the formation of a precipitate. Petroleum ether was evaporated, and **1d** was collected in 68.6% yield as a white powder with a melting point of 60−64 °C.

IR (neat) ν = 2953.87, 2822.95, 2764.52, 1709.96, 1567.03, 1468.08, 1264.86, 1220.38, 806.66 cm^{-1}; 1H NMR (400 MHz, $CDCl_3$) δ 8.11−8.09 (d, J = 8.8 Hz, 2H), 7.27−7.25 (d, J = 8.8 Hz, 2H), 4.40−4.37 (t, J = 6.4 Hz, 2H), 4.00 (s, 6H), 2.48−2.45 (t, J = 7.4 Hz, 2H), 2.29 (s, 6H), 2.00−1.93 (m, 2 H); ^{13}C NMR (100.42 MHz, DMSO-d_6) δ 174.5, 172.9, 165.8, 155.8, 131.8, 127.8, 122.9, 63.6, 56.4, 56.1, 45.5, 26.5. Calculated $C_{17}H_{22}N_4O_5$ ($[M + H]^+$), 362.4; found, 363.0.

*1-(Dimethylamino)propan-2-yl-4-((4,6-dimethoxy-1,3,5-triazin-2-yl)oxy)benzoate (**1e**).* Compound **1c** (2.0 g) was dissolved in 40 mL of dry THF. A solution of 6.76 mmol (0.94 mL) of dry triethylamine and 6.76 mmol (0.83 mL) of 1-dimethylamino-2-propanol in 10 mL of dry THF was added dropwise to the **1c** solution. Procedure B was

followed to provide **1e** in 41.6% yield as a white powder with a melting point of 48−52 °C.

IR (neat) ν = 2979.50, 2820.82, 2765.94, 1715.25, 1566.16, 1467.85, 1267.09, 1217.91, 806.42 cm^{-1}; ^1H NMR (400 MHz, $CDCl_3$) δ 8.11−8.09 (d, J = 8.8 Hz, 2 H), 7.27−7.25 (d, J = 8.8 Hz, 2 H), 5.38−5.30 (m, 1 H), 4.00 (s, 6H), 2.74−2.69 (dd, 1H), 2.49−2.44 (dd, 1H), 2.28 (s, 6 H), 1.38−1.36 (d, J = 6.4 Hz, 3H); ^{13}C NMR (100.42 MHz, DMSO-d_6) δ 174.0, 172.5, 165.6, 155.8, 131.6, 128.1, 122.8, 70.0, 64.4, 56.2, 46.8, 19.0. Calculated $C_{17}H_{22}N_4O_5$ ([M + H]$^+$), 362.4; found, 363.0.

*Bis(3-(dimethylamino)propan-yl)4,4′-((6-methoxy-1,3,5-triazine-2,4-diyl)bis(oxy))dibenzoate (**2d**).* Compound **2c**(2.0 g) (0.0048 mol) was dissolved in 55 mL of THF. Then, 1.32 mL of triethylamine and 0.0095 mols (1.13 mL) of 3-dimethylamino-1-propanol in 18.96 mL of THF were added to the **2c** solution in THF. Procedure B was followed to provide **2d** in 53.5% yield as a yellow powder with a melting point of 110−125 °C.

IR (neat) ν = 2948.39, 2856.39, 2768.09, 1710.28, 1578.14, 1466.51, 1268.23, 1207.71, 818.89 cm^{-1}; ^1H NMR (400 MHz, DMSO-d_6) δ 8.01−7.98 (d, J = 8.8 Hz, 4H), 7.26−7.24 (d, J = 8.8 Hz, 4H), 4.35−4.32 (t, 4H), 3.50−3.45 (t, 4H), 3.08 (s, 3H), 2.17 (s, 12H), 1.88−1.81 (m, 4H); ^{13}C NMR (100.42 MHz, DMSO-d_6) δ 172.8, 170.0, 166.0, 157.7, 131.5, 126.5, 123.0, 62.6, 56.0, 53.0, 45.5, 26.8. Calculated $C_{28}H_{35}N_5O_7$ ([M + H]$^+$), 553.7; found, 554.3.

*Bis(1-(dimethylamino)propan-2-yl)4,4′-((6-methoxy-1,3,5-triazine-2,4-diyl)bis(oxy))dibenzoate (**2e**).* Compound **2c** (2.0 g) (0.0048 mol) was dissolved in 55 mL of THF. Then, 1.32 mL of triethylamine and 0.009519 mols (1.126 mL) of 1-dimethylamino-2-propanol in 18.96 mL of THF was added to the **2c** solution in THF. Procedure B was followed to provide **2e** in 34.2% yield as a yellow powder with a melting point of 77−82 °C.

IR (neat) ν = 2976.79, 2822.66, 2766.79, 1710.21, 1556.42, 1469.03, 1265.37, 1208.40, 814.06 cm^{-1}; ^1H NMR (400 MHz, DMSO-d_6) δ 8.05−8.03 (d, J = 8.8 Hz, 4H), 7.29−7.27 (d, J = 8.8 Hz, 4H), 5.55−5.50 (m, 2H), 3.96−3.92 (dd, 2H), 3.69−3.66 (dd, 2H), 3.16 (s, 3H), 2.09 (s, 12H), 1.38−1.36 (d, J = 6.4 Hz, 6H); ^{13}C NMR (100.42 MHz, DMSO-d_6) δ 184.05, 180.47, 159.79, 157.57, 131.21, 125.87, 122.77, 66.24, 53.42, 45.90, 31.01, 19.06. Calculated $C_{28}H_{35}N_5O_7$ ([M + H]$^+$), 553.7; found, 554.3.

*2,4,6-Tris[(2′-dimethylamino-1′-ethoxy)-4′-]-1,3,5-triazine (**3d**).* Compound **3c** (3.0 g) (5.51 mmol) was dissolved in 60 mL of dry THF at room temperature conditions. A solution of 2.3 mL of 2-dimethylaminoethanol and 2.5 mL of triethylamine in 10 mL of dry THF was added dropwise to the **3c** solution. Procedure B was followed, however, with the temperature for the reaction maintained at 15 °C. Compound **3d** had a melting point of 85−87 °C and a final yield of 17%.

IR (neat) ν = 2968.08, 2944.40, 2819.10, 2768.72, 1715.44, 1598.22, 1567.52, 1500.82, 1461.87, 1411.07, 1362.17, 1270.29, 1207.95, 1114.66, 1014.66, 861.27; ^1H NMR (400 MHz, DMSO-d_6) δ 8.01−7.99 (d, J = 8.8 Hz, 6H); 7.42−7.40 (d, J = 8.8 Hz, 6H), 4.38−4.36 (t, J = 5.6 Hz, 6H), 2.67−2.65 (t, J = 5.6 Hz, 6H), 2.24 (s, 18H); ^{13}C NMR (100.42 MHz, DMSO-d_6) δ 173.3, 166.1, 155.0, 131.8, 128.2, 122.6, 62.9, 57.5, 46.0. Calculated $C_{36}H_{42}N_6O_9$ ([M + H]$^+$), 702.9; found, 703.3.

*2,4,6-Tris[(1′-dimethylamino-2′-propoxy)-4′-carbonylphenoxy]-1,3,5-triazine (**3e**).* Compound **3c** (1.3 g) (2.39 mmol) was dissolved in 60 mL of dry THF at room temperature conditions. A solution of 0.725 g (7.16 mmol) of 1-dimethylamino-2-propanol and 0.725 g (7.16 mmol) of triethylamine in 10 mL of dry THF was added dropwise to the **3c** solution under anhydrous conditions. Procedure B was followed with temperature maintained at 40 °C to provide **3e** in 64.4% yield as a white powder with a melting point of 76−82 °C.

IR (neat) ν = 2976.71, 2945.91, 2821.90, 2771.82, 1713.27, 1604.26, 1562.07, 1501.56, 1266.04, 1201.13, 1159.69, 1113.14, 1013.70, 810.92 cm^{-1}; ^1H NMR (400 MHz, DMSO-d_6) δ 8.01−7.99 (d, J = 8.8 Hz, 6H), 7.42−7.40 (d, J = 8.8 Hz, 6H), 5.5−5.19 (m, 3H), 2.67−2.63 (dd, 3H), 2.44−2.44 (dd, 6H), 2.24 (s, 18H), 1.30−1.28 (d, J = 6.3, 9H); ^{13}C NMR (100.42 MHz, DMSO-d_6) δ 172.6, 164.7, 153.4, 131.3, 128.4, 122.3, 69.5, 63.7, 46.0, 19.1. Calculated $C_{39}H_{48}N_6O_9$ ([M + H]$^+$), 745.0; found, 745.4.

Procedure for *sym*-Triazine Based Iodine-Ester Salts. *3-((4-((4,6-Dimethoxy-1,3,5-triazin-2-yl)oxy)benzoyl)oxy)-N,N,N-trimethylpropan-1-aminium iodide (**1f**) (Procedure C).* Iodomethane (2.06 mL) (0.033 mol) was added dropwise to a solution of 1.20 g (3.3 mmol) of **1d** in 40 mL of dry THF. The mixture was stirred for 2 h at 40 °C and left overnight under dry conditions. The resulting precipitate was filtered and washed by 2 × 6 mL of dry THF and 2 × 10 mL of petroleum ether to provide **1f** in 88.0% yield as a white powder with a melting point of 176−179 °C.

IR (neat) ν = 3002.94, 2954.31, 1717.40, 1554.68, 1459.01, 1266.75, 1215.76, 815.41 cm^{-1}; ^1H NMR (400 MHz, D_2O) δ 8.02−8.01 (d, J = 8.9 Hz, 2H), 7.27−7.25 (d, J = 8.9 Hz, 2H), 4.37−4.35 (t, 2H), 3.88 (s, 6H), 3.46−3.43 (t, 2 H), 3.06 (s, 6H), 2.28−2.20 (m, 2 H); ^{13}C NMR (100.42 MHz, D_2O) δ 173.6, 172.7, 167.6, 155.5, 131.6, 126.7, 122.2, 64.3, 62.5, 56.4, 53.3, 22.7. Calculated $C_{18}H_{25}N_4O_5$ ([M + H]$^+$), 377.3; found, 377.2.

*3-((4-((4,6-Dimethoxy-1,3,5-triazin-2-yl)oxy)benzoyl)oxy)-N,N,N,2-trimethylpropan-1-aminium Iodide (**1g**).* Iodomethane (1.60 mL) (0.025 mol) was added dropwise to a solution of 0.92 g (0.0025 mol) of **1e** in 40 mL of dry THF. Procedure C was followed to provide **1g** in 74.2% yield as a white powder with a melting point of 188−191 °C.

IR (neat) ν = 2997.32, 2952.72, 1721.29, 1558.83, 1467.22, 1256.47, 1220.57, 810.91 cm^{-1}; ^1H NMR (400 MHz, D_2O) δ 8.05−8.03 (d, J = 8.8 Hz, 2H), 7.27−7.25 (d, J = 8.8 Hz, 2H), 5.64−5.56 (m, 1H), 3.93−3.89 (dd, 1H), 4.65 (s, 6H), 3.47−3.42 (dd, 1H), 3.11 (s, 9H), 1.36−1.34 (d, J = 6.43 Hz, 3H); ^{13}C NMR (100.42 MHz, D_2O) δ 173.6, 172.7, 166.2, 155.8, 132.0, 127.5, 122.2, 67.6, 56.2, 54.2, 54.1, 19.0. Calculated $C_{18}H_{25}N_4O_5$ ([M + H]$^+$), 377.3; found, 377.2.

*3,3′-((4,4′-((6-Methoxy-1,3,5-triazine-2,4-diyl)bis(oxy))bis-(benzoyl))bis(oxy))bis(N,N,N-trimethylpropan-1-aminium) Iodide (**2f**).* Iodomethane 0.38 mL (6.1 mmol) was added dropwise to a solution of 1.3 mmol of **2d** in 34.6 mL of THF. Procedure C was followed to provide **2f** in 38.7% yield as a yellow powder with a melting point of 180−185 °C.

IR (neat) ν = 3014.25, 2956.28, 1710.56, 1559.66, 1476.14, 1271.12, 1208.75, 821.05 cm^{-1}; ^1H NMR (400 MHz, D_2O) δ 7.84−7.82 (d, J = 8.8 Hz, 4H), 7.19−7.17 (d, J = 8.8 Hz, 4H), 4.33−4.29 (t, 4H), 3.8 (s, 3H), 3.65−3.61 (t, 4H), 3.01 (s, 18H), 1.78−1.74 (m, 2H) ; ^{13}C NMR (100.42 MHz, D_2O) δ 181.2, 180.1, 167.3, 155.7, 131.6, 127.1, 122.2, 68.0, 64.0, 53.3, 53.0, 22.5. Calculated $C_{30}H_{41}N_5O_7$ ([M + 2H]$^{2+}$), 291.9; found, 291.7.

*2,2′-((4,′4-((6-Methoxy-1,3,5-triazine-2,4-diyl)bis(oxy))bis-(benzoyl))bis(oxy))bis(N,N,N-trimethylpropan-1-aminium) Iodide (**2g**).* Iodomethane (0.38 mL) (6.1 mmol) was added dropwise to the solution of 1.3 mmol of **2e** in 34.6 mL of THF. Procedure C was followed to provide **2g** in 44.4% yield as a yellow powder with a melting point of 205−210 °C.

IR (neat) ν = 3007.65, 2958.47, 1709.58, 1560.48, 1498.38, 1264.01, 1210.11, 765.47 cm^{-1}; ^1H NMR (400 MHz, DMSO-d_6) δ 8.13−8.11 (d, J = 8.5 Hz, 4H), 7.48−7.46 (d, J = 8.5 Hz, 4H), 5.56−5.50 (m, 2H), 3.98−3.94 (dd, 2H), 3.72−3.69 (dd, 2H), 3.18 (s, 3H), 2.09 (s, 18H), 1.39−1.37 (d, J = 6.3 Hz, 6H); ^{13}C NMR (100.42 MHz, DMSO-d_6) δ 180.06, 176.57, 174.34, 164.18, 131.60, 127.17, 121.33, 68.47, 66.71, 53.43, 19.50. Calculated $C_{30}H_{41}N_5O_7$ ([M + 2H]$^{2+}$), 291.9; found, 291.7.

*2,4,6-Tris[iodomethylate(2′-trimethylamino-1′-ethoxy)-4′-carbonylphenoxyl 1,3,5-triazine (**3f**).* Compound **3d** (0.62 g) (0.88 mmol) was purified and dissolved in 45 mL of dry THF at room temperature conditions. Separately, 0.4 mL (6.2 mmol) of methyl iodide was dissolved in 15 mL of THF and stirred for 3 h. Procedure C was followed to provide **3f** with a melting point >185 °C with decomposition and a final yield of 68.0%.

IR (neat) ν = 3043.00, 3005.74, 2956.78, 1717.44, 1593.83, 1567.08, 1502.23, 1265.59, 1209.07, 1163.95, 1113.80, 1012.95, 808.38 cm^{-1}; ^1H NMR (400 MHz, DMSO-d_6) δ 8.10−8.08 (d, J = 8.8 Hz, 6H); 7.47−7.45 (d, J = 8.8 Hz, 6H), 4.74−4.73 (t, 6H); 3.85−3.83 (t, 6H), 3.23 (s, 27H); ^{13}C NMR (100.42 MHz, DMSO-d_6) δ 173.06, 165.08,

155.43, 131.66, 127.24, 122.32, 64.48, 59.21, 53.47. Calculated $C_{39}H_{51}N_6O_9$ ([M + H]$^+$), 748.0; found, 749.0.

*2,4,6-Tris[iodomethylate(1′-trimethylamino-2′-propoxy)-4′-carbonylphenoxyl 1,3,5-triazine (**3g**).* Methyl iodine (0.65 mL) (10.6 mmol) was added dropwise into a 1.16 g (1.56 mmol) solution of **3e** in 40 mL of dry THF at room temperature conditions. Procedure C was followed to provide **3g** as a light yellow powder with a 189−191 °C melting point and final yield of 89.1%.

IR (neat) ν = 3036.05, 2998.40, 2974.64, 1713.58, 1592.99, 1565.76, 1501.62, 1262.78, 1206.61, 1162.67, 1093.84, 1013.10; ^{1}H NMR (400 MHz, DMSO-d_6) δ 8.12−8.10 (d, J = 8.8 Hz, 6H), 7.47−7.45 (d, J = 8.8 Hz, 6H); 5.56−5.50 (m, 3H), 3.98−3.93 (dd, 3H), 3.72−3.69 (dd, 3H), 3.30 (s, 27H); 1.39−1.37 (d, J = 6.0 Hz, 9H); ^{13}C NMR (100.42 MHz, DMSO-d_6) δ 173.09, 164.23, 155.59, 131.69, 127.62, 122.68, 68.38, 66.92, 53.69, 19.03. Calculated $C_{42}H_{57}N_6O_9$ ([M + H]$^+$), 790.1; found, 791.2.

Pretreatment for Amyloid Monomerization. Human Aβ_{1-40} Gln11 trifluoroacetate salt (EMD4Biosciences; Gibbstown, NJ) was dissolved in neat HFIP at a ratio of 1 mg:1 mL. Cloudy suspensions were sonicated for 15 min until samples became clear. Aβ_{1-40}/HFIP solutions were shaken at 400 rpm for 2 h at 4 ± 1 °C. The samples were left in HFIP and sealed overnight. HFIP was then removed by nitrogen bubbling, leaving a clear thin film. Samples were then stored at −20 °C until needed and reconstituted in DMSO, followed by dilution to the appropriate concentrations with 50 mM phosphate buffered saline (PBS), and 100 mM NaCl at pH 7.4. ThT stock (10 mM) was prepared in 18.2 MΩ water and stored in aluminum foil. Peptide concentrations were determined by measuring the OD at 280 nm (ε_{280} = 1280 M^{-1}) using NanoDrop 2000 (ThermoScientific, Mississauga, ON).

ThT Fluorescence. Fluorescence measurements were conducted in black optilux fluorescence 96-well plates (BD Biosciences, Mississauga, Canada) using a Synergy HT Multimode Microplate reader from BioTek (Winooski, VT). Each 200 μL sample well contained ThT (100 μM) and Aβ_{1-40} (100 μM) in the presence of 0 μM, 50 μM, 100 μM, or 200 μM of the tested inhibitor. Spontaneous aggregation of amyloid samples was induced by incubation at 37 ± 1 °C with shaking at 300 rpm. Sample fluorescence (λ_{EX} 440 nm; λ_{EM} 485 nm) was recorded at various time intervals over 72 h ($n \geq 3$).

Transmission Electron Microscopy Studies. An aliquot (6 μL) of Aβ_{1-40} samples was spotted onto nickel Formvar mesh grids (Electron Microscopy Sciences, Hatfield, PA) for 1 min and blot dried. The TEM grids were subsequently stained using 6 μL of 1% uranyl acetate for 1 min followed by blot drying. Samples were imaged using a Hitachi H-7500 transmission electron microscope.[46,53]

Inhibition Assays for AChE and BuChE. The influence of *sym*-triazine compounds on the hydrolytic activity of human erythrocyte AChE (Sigma-Aldrich; Oakville, ON) was determined using Ellman's method.[22,40,41] Enzyme assay solutions were prepared in a microplate well containing AChE (0.1875 U/mL) and DTNB (340 μM) in 0.1 M PBS at pH 8.0 at 37 ± 1 °C. The enzyme reaction was initiated by the addition of acetylthiocholine iodide (0.550 μM). Optical density at 410 nm was measured in 15 s intervals for a period of 5 min using a Synergy HT Multimode Microplate reader. The initial reaction rate ($OD_{410\ nm}$/min) was determined from linear regression analysis of the absorbance time curves (n = 3). The rate of the uninhibited enzyme hydrolysis (V_o) was calibrated to 0.100 $OD_{410\ nm}$/min ± 0.030. The reaction rate was then measured in the presence of inhibitors (V_i) at various concentrations. AChE activity was determined by the expression % AChE Activity = (V_i/V_o) × 100. For each inhibitor, the enzyme activity was plotted as a function of the logged concentration. Nonlinear regression of inhibition plots was performed to determine the IC_{50} concentration. BuChE inhibition studies were performed as previously described, using 0.350 U·mL^{-1} of BuChE and 0.550 μM butyrylthiocholine iodide substituted for the active enzyme and substrate, respectively.

To determine the competitive inhibition constant, K_i, the initial reaction velocities of **2g**, **3d**, **3f**, and **3g** at various concentrations were measured over a range of low ATChI substrate concentration (550, 225, 112, and 56 μM) and evaluated by a double reciprocal plot. For each inhibitor concentration, a linear slope showing the reciprocal of initial velocity and substrate concentration was measured. K_i was determined from replots of the slope data versus inhibitor concentration, wherein the K_i value was denoted by the x-intercept extrapolated by least-squares analysis.

Cell Culture, Differentiation, and Treatment. The human SH-SY5Y neuronal cell line (American Type Culture Collection, Manassas, VA) was maintained in Dulbecco's modified Eagle's medium (DMEM) supplemented with 10% fetal bovine serum (FBS). Cultures were maintained at 37 °C in a humidified 5% CO_2 atmosphere. After plating at a cell density of 4.4 × 10^4 cells per cm^2 and allowing for cell adhesion for 24 h, neuronal differentiation was induced by treatment using 10 μM of all-*trans*-retinoic acid at 37 °C for 72 h under serum-free conditions.[54]

Cell Viability Studies. The quantitative assay for the viability of differentiated human neuronal cells employed the propidium iodide ([PI], Sigma Aldrich, St Louis, MO, USA) exclusion methodology. Samples (2 × 10^4 cells per well) were plated in 96-well plates with eight replicates, treated with various concentrations of **3f** or **3g** as indicated for 24 h.[55] PI was used as a viability dye (10 μg/mL) and 300 nM 4′,6-diamidino-2-phenylindole (DAPI) (Invitrogen, Carlsbad CA, USA) as a counter stain for nuclei. PI fluorescence was measured by a FLUOstar OPTIMA microplate reader (BMG Labtech, Offenburg, Germany) set to fluorescence mode with an excitation wavelength of 544 nm and an emission wavelength of 612 nm. Healthy cells that retained the membrane integrity were stained blue by DAPI while being able to exclude PI. Dead cells (late apoptotic or necrotic) were PI positive due to a loss of membrane integrity. Cell death of differentiated human neuronal cells was induced by treatment with a toxic dosage of celastrol (3 μM) as previously reported for use as a positive control.[55] Cell viability was further confirmed by examination of cellular morphology with phase contrast and epifluorescence (DAPI counter staining) microscopy. Cells were fixed with 4% paraformaldehyde followed by permeabilization with 0.1% Triton X-100. Dying cells showed extensive rounding of the cell body and condensation of nuclei.

■ ASSOCIATED CONTENT

Supporting Information

Steady-state inhibition of AChE by *sym*-triazine derivatives **2g**, **3d**, **3f**, and **3g**; transmission electron micrographs depicting inhibited fibril formation of Aβ_{1-40}; ^{1}H-NMR of *sym*-triazine derivatives; and ^{13}C-NMR of *sym*-triazine derivatives. This material is available free of charge via the Internet at http://pubs.acs.org.

■ AUTHOR INFORMATION

Corresponding Author

*Tel: +1 416 287 7250. Fax: +1 416 287 7279. E-mail: kagan.kerman@utoronto.ca.

Author Contributions

[§]These authors contributed equally to the preparation of this manuscript.

Funding

This research was carried out with the financial support of NSERC Discovery Grants to K.K. and I.R.B., a Biomedical Young Investigator Award from the Alzheimer Society of Canada to K.K., and a Canada Research Chair (Tier I) in Neuroscience to I.R.B.

Notes

The authors declare no competing financial interest.

■ ACKNOWLEDGMENTS

We thank Professor Mauricio Terebiznik and Darren Gigliozzi (University of Toronto Scarborough, Department of Biological

Sciences) for their technical assistance in ThT fluorescence studies and Robert Temkin for his aid with transmission electron microscopy imaging. We also acknowledge Leayen B. Lam for her assistance with cholinesterase activity measurements.

REFERENCES

(1) Lesne, S., Koh, M. T., Kotilinek, L., Kayed, R., Glabe, C. G., Yang, A., Gallagher, M., and Ashe, K. H. (2006) A specific amyloid-beta protein assembly in the brain impairs memory. *Nature 440*, 352−357.

(2) Buckner, R. L., Snyder, A. Z., Shannon, B. J., LaRossa, G., Sachs, R., Fotenos, A. F., Sheline, Y. I., Klunk, W. E., Mathis, C. A., Morris, J. C., and Mintun, M. A. (2005) Molecular, structural, and functional characterization of Alzheimer's disease: Evidence for a relationship between default activity, amyloid, and memory. *J. Neurosci. 25*, 7709−7717.

(3) Small, G. W., Kepe, V., Ercoli, L. M., Siddarth, P., Bookheimer, S. Y., Miller, K. J., Lavretsky, H., Burggren, A. C., Cole, G. M., Vinters, H. V., Thompson, P. M., Huang, S. C., Satyamurthy, N., Phelps, M. E., and Barrio, J. R. (2006) PET of brain amyloid and tau in mild cognitive impairment. *New. Engl. J. Med. 355*, 2652−2663.

(4) Davies, R. R., Hodges, J. R., Kril, J. J., Patterson, K., Halliday, G. M., and Xuereb, J. H. (2005) The pathological basis of semantic dementia. *Brain 128*, 1984−1995.

(5) Querfurth, H. W., and LaFerla, F. M. (2010) Mechanisms of disease: Alzheimer's disease. *New. Engl. J. Med. 362*, 329−344.

(6) Zheng, L., Kagedal, K., Dehvari, N., Benedikz, E., Cowburn, R., Jan, M., and Terman, A. (2009) Oxidative stress induces macroautophagy of amyloid beta-protein and ensuing apoptosis. *Free Radical Biol. Med. 46*, 422−429.

(7) Demuro, A., Mina, E., Kayed, R., Milton, S. C., Parker, I., and Glabe, C. G. (2005) Calcium dysregulation and membrane disruption as a ubiquitous neurotoxic mechanism of soluble amyloid oligomers. *J. Biol. Chem. 280*, 17294−17300.

(8) Qin, L. Y., Liu, Y. X., Cooper, C., Liu, B., Wilson, B., and Hong, J. S. (2002) Microglia enhance beta-amyloid peptide-induced toxicity in cortical and mesencephalic neurons by producing reactive oxygen species. *J. Neurochem. 83*, 973−983.

(9) Geng, J., Li, M., Ren, J. S., Wang, E. B., and Qu, X. G. (2011) Polyoxometalates as inhibitors of the aggregation of amyloid beta peptides associated with Alzheimer's disease. *Angew. Chem., Int. Ed. 50*, 4184−4188.

(10) Wang, H.-Y., Ying, Y.-L., Li, Y., Kraatz, H.-B., and Long, Y.-T. (2011) Nanopore analysis of beta-amyloid peptide aggregation transition induced by small molecules. *Anal. Chem. 83*, 1746−1752.

(11) Rinne, J. O., Brooks, D. J., Rossor, M. N., Fox, N. C., Bullock, R., Klunk, W. E., Mathis, C. A., Blennow, K., Barakos, J., Okello, A. A., de Llano, S. R. M., Liu, E., Koller, M., Gregg, K. M., Schenk, D., Black, R., and Grundman, M. (2010) (11)C-PiB PET assessment of change in fibrillar amyloid-beta load in patients with Alzheimer's disease treated with bapineuzumab: a phase 2, double-blind, placebo-controlled, ascending-dose study. *Lancet Neurol. 9*, 363−372.

(12) Siemers, E. R., Friedrich, S., Dean, R. A., Gonzales, C. R., Farlow, M. R., Paul, S. M., and DeMattos, R. B. (2010) Safety and changes in plasma and cerebrospinal fluid amyloid beta after a single administration of an amyloid beta monoclonal antibody in subjects with Alzheimer disease. *Clin. Neuropharmacol. 33*, 67−73.

(13) Raina, P., Santaguida, P., Ismaila, A., Patterson, C., Cowan, D., Levine, M., Booker, L., and Oremus, M. (2008) Effectiveness of cholinesterase inhibitors and memantine for treating dementia: Evidence review for a clinical practice guideline. *Ann. Intern. Med. 148*, 379−397.

(14) Schliebs, R., and Arendt, T. (2006) The significance of the cholinergic system in the brain during aging and in Alzheimer's disease. *J. Neural. Trans. 113*, 1625−1644.

(15) Daiello, L. A. (2007) Current issues in dementia pharmacotherapy. *Am. J. Manag. Care 13*, S198−S202.

(16) Delrieu, J., Piau, A., Caillaud, C., Voisin, T., and Vellas, B. (2011) Managing cognitive dysfunction through the continuum of Alzheimer's disease role of pharmacotherapy. *CNS Drugs 25*, 213−226.

(17) Bassil, N., and Grossberg, G. T. (2009) Novel regimens and delivery systems in the pharmacological treatment of Alzheimer's disease. *CNS Drugs 23*, 293−307.

(18) Watkins, P. B., Zimmerman, H. J., Knapp, M. J., Gracon, S. I., and Lewis, K. W. (1994) Hepatotoxic effects of tacrine administration in patients with Alzheimer's disease. *J. Am. Med. Assoc. 271*, 992−998.

(19) Inestrosa, N. C., Alvarez, A., Perez, C. A., Moreno, R. D., Vicente, M., Linker, C., Casanueva, O. I., Soto, C., and Garrido, J. (1996) Acetylcholinesterase accelerates assembly of amyloid-beta-peptides into Alzheimer's fibrils: Possible role of the peripheral site of the enzyme. *Neuron 16*, 881−891.

(20) Onor, M. L., Trevisiol, M., and Aguglia, E. (2007) Rivastigmine in the treatment of Alzheimer's disease: An update. *Clin. Interventions Aging 2*, 17−32.

(21) Lane, R. M., Kivipelto, M., and Greig, N. H. (2004) Acetylcholinesterase and its inhibition in Alzheimer disease. *Clin. Neuropharmacol. 27*, 141−149.

(22) Piazzi, L., Rampa, A., Bisi, A., Gobbi, S., Belluti, F., Cavalli, A., Bartolini, M., Andrisano, V., Valenti, P., and Recanatini, M. (2003) 3-(4-{Benzyl(methyl)amino methyl}-phenyl)-6,7-dimethoxy-2H-2-chromenone (AP2238) inhibits both acetylcholinesterase and acetylcholinesterase-induced beta-amyloid aggregation: A dual function lead for Alzheimer's disease therapy. *J. Med. Chem. 46*, 2279−2282.

(23) Dantoine, T., Auriacombe, S., Sarazin, M., Becker, H., Pere, J. J., and Bourdeix, I. (2006) Rivastigmine monotherapy and combination therapy with memantine in patients with moderately severe Alzheimer's disease who failed to benefit from previous cholinesterase inhibitor treatment. *Int. J. Clin. Pract. 60*, 110−118.

(24) Morphy, R., and Rankovic, Z. (2005) Designed multiple ligands. An emerging drug discovery paradigm. *J. Med. Chem. 48*, 6523−6543.

(25) Bolognesi, M. L., Cavalli, A., and Melchiorre, C. (2009) Memoquin: A multi-target-directed ligand as an innovative therapeutic opportunity for Alzheimer's disease. *Neurotherapeutics 6*, 152−162.

(26) Cavalli, A., Bolognesi, M. L., Minarini, A., Rosini, M., Tumiatti, V., Recanatini, M., and Melchiorre, C. (2008) Multi-target-directed ligands to combat neurodegenerative diseases. *J. Med. Chem. 51*, 347−372.

(27) Rosini, M., Simoni, E., Bartolini, M., Cavalli, A., Ceccarini, L., Pascu, N., McClymont, D. W., Tarozzi, A., Bolognesi, M. L., Minarini, A., Tumiatti, V., Andrisano, V., Mellor, I. R., and Melchiorre, C. (2008) Inhibition of acetylcholinesterase, beta-amyloid aggregation, and NMDA receptors in Alzheimer's disease: A promising direction for the multi-target-directed ligands gold rush. *J. Med. Chem. 51*, 4381−4384.

(28) Bolognesi, M. L., Bartolini, M., Rosini, M., Andrisano, V., and Melchiorre, C. (2009) Structure-activity relationships of memoquin: Influence of the chain chirality in the multi-target mechanism of action. *Bioorg. Med. Chem. Lett. 19*, 4312−4315.

(29) Piazzi, L., Cavalli, A., Colizzi, F., Belluti, F., Bartolini, M., Mancini, F., Recanatini, M., Andrisano, V., and Rampa, A. (2008) Multi-target-directed coumarin derivatives: hAChE and BACE1 inhibitors as potential anti-Alzheimer compounds. *Bioorg. Med. Chem. Lett. 18*, 423−426.

(30) Choi, K. Y., Swierczewska, M., Lee, S., and Chen, X. (2012) Protease-activated drug development. *Theranostics 2*, 156−178.

(31) Elderfield, R. C. (1961) Heterocyclic Compounds, in *Polycyclic Compounds Containing Two Hetero Atoms in Different Rings* (Elderfield, R. C., Ed.), 1st ed., John Wiley and Sons, New York.

(32) Gupta, R. R., Kumar, M., and Gupta, V. (1999) In *Heterocyclic Chemistry* (Gupta, R. R., Ed.), 1st ed., Springer, New York.

(33) Mur, V. I. (1964) 2,4,6-Trichloro-1,3,5-triazine (cyunaryl chloride) and its future applications. *Russ. Chem. Rev. 33*, 92−103.

(34) Blotny, G. (2006) Recent applications of 2,4,6-trichloro-1,3,5-triazine and its derivatives in organic synthesis. *Tetrahedron 62*, 9507−9522.

(35) Thurston, J. T., Dudley, J. R., Kaiser, D. W., Hechenbleikner, I., Schaefer, F. C., and Holmhansen, D. (1951) Cyunaric chloride derivatives 0.1. Aminochloro-s-triazines. *J. Am. Chem. Soc. 73*, 2981−2983.
(36) Afonso, C. A. M., Lourenco, N. M. T., and Rosatella, A. D. (2006) Synthesis of 2,4,6-tri-substituted-1,3,5-triazines. *Molecules 11*, 81−102.
(37) Dudley, J. R., Thurston, J. T., Schaefer, F. C., Holmhansen, D., Hull, C. J., and Adams, P. (1951) Cyunaric chloride derivatives 0.3. Alkoxy-s-triazines. *J. Am. Chem. Soc. 73*, 2986−2990.
(38) Pogosyan, G. M., Zaplishnyi, V. I., Khachatryan, M. A., and Atashyan, S. M. (1986) Synthesis of an iron-ammonia complex of an acid containing s-triazine and production of thermostable adhesives from it. *J. App. Chem. USSR 59*, 588−593.
(39) Sklyarskii, L. S., Akopyan, L. L., Ogandzhanyan, L. M., Stepanyan, V. N., Zaplishny, V. N., and Pogosyan, G. M. (1988) Polymerklei Scientific-Industrial Enterprisess USSR, U.S.S.R. Published Patent Application SU 1409629.
(40) Ellman, G. L., Courtney, K. D., Andres, V., and Featherstone, R. M. (1961) A new and rapid colorimetric determination of acetylcholinesterase activity. *Biochem. Pharmacol. 7*, 88.
(41) Rampa, A., Bisi, A., Belluti, F., Gobbi, S., Valenti, P., Andrisano, V., Cavrini, V., Cavalli, A., and Recanatini, M. (2000) Acetylcholinesterase inhibitors for potential use in Alzheimer's disease: Molecular modeling, synthesis and kinetic evaluation of 11H-indeno- 1,2-b -quinolin-10-ylamine derivatives. *Bioorg. Med. Chem. 8*, 497−506.
(42) Jackisch, R., Foerster, S., Kammerer, M., Rothmaier, A. K., Ehret, A., Zentner, J., and Feuerstein, T. J. (2009) Inhibitory potency of choline esterase inhibitors on acetylcholine release and choline esterase activity in fresh specimens of human and rat neocortex. *J. Alzheimer's Dis. 16*, 635−647.
(43) Barak, D., Ordentlich, A., Bromberg, A., Kronman, C., Marcus, D., Lazar, A., Ariel, N., Velan, B., and Shafferman, A. (1995) Allosteric modulation of acetylcholinesterase activity by peripheral ligands involves a conformational transition of the anionic subsite. *Biochemistry 34*, 15444−15452.
(44) Massoulie, J., Sussman, J., Bon, S., and Silman, I. (1993) Cholinergic Function and Dysfunction, in *Structure and Functions of Acetylcholinesterase and Butyrylcholinesterase* (Cuello, A. C., Ed.), 1st ed., pp 139−146, Elsevier Science Publishers, Amsterdam.
(45) Sun, Y., Zhang, G., Hawkes, C. A., Shaw, J. E., McLaurin, J., and Nitz, M. (2008) Synthesis of scyllo-inositol derivatives and their effects on amyloid beta peptide aggregation. *Bioorgan. Med. Chem. 16*, 7177−7184.
(46) Wong, H. E., Qi, W., Choi, H.-M., Fernandez, E. J., and Kwon, I. (2011) A safe, blood-brain barrier permeable triphenylmethane dye inhibits amyloid-β neurotoxicity by generating nontoxic aggregates. *ACS Chem. Neurosci. 2*, 645−657.
(47) Estrada, L. D., and Soto, C. (2007) Disrupting beta-amyloid aggregation for Alzheimer disease treatment. *Curr. Top. Med. Chem. 7*, 115−126.
(48) Haass, C., and Selkoe, D. J. (2007) Soluble protein oligomers in neurodegeneration: lessons from the Alzheimer's amyloid beta-peptide. *Nature Rev. Mol. Cell Biol. 8*, 101−112.
(49) Bieschke, J., Russ, J., Friedrich, R. P., Ehrnhoefer, D. E., Wobst, H., Neugebauer, K., and Wanker, E. E. (2010) EGCG remodels mature alpha-synuclein and amyloid-beta fibrils and reduces cellular toxicity. *Proc. Natl. Acad. Sci. U.S.A. 107*, 7710−7715.
(50) Ehrnhoefer, D. E., Bieschke, J., Boeddrich, A., Herbst, M., Masino, L., Lurz, R., Engemann, S., Pastore, A., and Wanker, E. E. (2008) EGCG redirects amyloidogenic polypeptides into unstructured, off-pathway oligomers. *Nat. Struct. Mol. Biol. 15*, 558−566.
(51) Meng, X., Munishkina, L. A., Fink, A. L., and Uversky, V. N. (2009) Molecular mechanisms underlying the flavonoid-induced inhibition of alpha-synuclein fibrillation. *Biochemistry 48*, 8206−8224.
(52) LeVine, H. (2004) The Amyloid Hypothesis and the clearance and degradation of Alzheimer's beta-peptide. *J. Alzheimer's Dis. 6*, 303−314.
(53) Chi, E. Y., Frey, S. L., Winans, A., Lam, K. L. H., Kjaer, K., Majewski, J., and Lee, K. Y. C. (2010) Amyloid-beta fibrillogenesis seeded by interface-induced peptide misfolding and self-assembly. *Biophys. J. 98*, 2299−2308.
(54) Xie, H. R., Hu, L. S., and Li, G. Y. (2010) SH-SY5Y human neuroblastoma cell line: in vitro cell model of dopaminergic neurons in Parkinson's disease. *Chinese Med. J. 123*, 1086−1092.
(55) Chow, A. M., and Brown, I. R. (2007) Induction of heat shock proteins in differentiated human and rodent neurons by celastrol. *Cell Stress Chaperones 12*, 237−244.